Numerical approach to the lateral buckling of steel tied-arch bridges

A. Outtier, H. De Backer and Ph. Van Bogaert
Ghent University, Civil Engineering Department, Belgium

ABSTRACT: Detailed finite element models of several steel tied-arch bridges are used for the calculation of the lateral buckling strength. Each detail, including the arch diaphragms and stiffeners, the deck plate and bearings, is conscientiously modelled. Several out-of-plane imperfections are superposed on the finite element model of the bridge. This model is used for the calculation of the critical elastic out-of-plane buckling force and with a slight modification for the calculation of the critical plastic out-of-plane buckling force. Based on these values, the resistance towards out-of-plane buckling can be calculated. The results of these calculations are finally compared to the existing buckling curves for straight beams, as mentioned in the Eurocodes. The main conclusion of this comparison is that the out-of-plane buckling behaviour of arches is less critical, than it seems to be, when calculated using buckling curves for of a straight beam with the same section.

1 INTRODUCTION

The fundamental behaviour of tied-arches is based on the fact that a large compressive force is developed in the arch cross-section. Because of this, steel arches in particular can become highly sensitive to the out-of-plane buckling phenomenon. However, there is no clear and generally accepted calculation method to predict numerically this stability problem. On one hand, the buckling strength of a steel tied-arch bridge can be calculated by considering the non-linear elastic-plastic behaviour. As the imperfections of the arches highly influence the non-linear behaviour, these geometrical imperfections need to be known before starting this analysis. On the other hand, a linear calculation, resulting in an elastic buckling factor for the compression force, can be carried out. A multiplication factor for the occurring stresses can be found based on this calculation, using an adequate buckling curve, as mentioned for straight beams in ECCS-EG77-2E (1978). In this case of proceeding by buckling curves, as well, the arch imperfections should be known beforehand. However, the imperfections in slender steel arch bridges are not related to those of a straight beam or column which makes it fundamentally impossible, or at least overly safe, to use the standard buckling curves, derived for straight beams.

To improve the knowledge in this research field, several steel tied-arch bridges have been equipped with strain gauges, as shown by Van Bogaert and Outtier (2006), at various relevant cross-sections of the arch, spread out evenly along the total length of the arch. The size and shape of the out-of-plane geometrical imperfections were thus derived for these bridges using an analytical calculation method, described in Outtier et al (2006).

In the linear elastic, as well as in the elastic-plastic calculation, the influence of these geometrical out-of-plane imperfections on the lateral buckling behaviour are simulated, using a highly detailed finite element model. As the imperfections of arch bridges are smaller than can be expected for straight members, every detail of the bridge becomes important for determining the buckling load and may influence the results of the numerical simulations. Therefore, all details,

such as diaphragms, connection plates, orthotropic plated bridge deck, bearing systems and arch springs, are modelled in a very exact manner for the calculations which are the basis of this research paper.

Forthcoming of these calculations and of the quantification of the geometrical imperfections, the application of a similar finite element model allows for calculating the resistance to out-of-plane buckling of steel arches. This calculation method constitutes the main contribution of this paper.

2 DESCRIPTION OF THE FINITE ELEMENT MODEL

A finite element model of the Albert Canal Bridge, which can be seen in Fig. 1, is used as the basis for the research on the resistance to out-of-plane buckling of arches. The Albert Canal Bridge was recently built in Belgium near the city of Antwerp, as part of the new high speed railway between Antwerp and Amsterdam. The bridge span equals 115 m, which is quite larger than the Albert Canal itself. However, this bridge span has been chosen in view of the further widening of the canal and the increasing of fluvial traffic on the canal toward the Port of Antwerp. The two arches of this steel tied-arch bridge are connected to the lower chord members by sixteen inclined hangers. The upper bracing is formed by three tubes of large diameters spread out along the length of the arch. The arch springs are tied by the lower chord, consisting of an orthotropic steel deck plate. The bridge is supported by neoprene bearing systems.

Figure 1: The Albert Canal Bridge

The finite element model, developed for this bridge can be seen in Fig. 2. To obtain a model that is as accurate as possible, special attention is given to all the details of the bridge, as is being described further, especially those which might introduce asymmetry into the model or might influence the buckling behaviour. Several possible out-of-plane imperfections are then superposed on the model of the bridge, to assess their influence on the buckling behaviour.
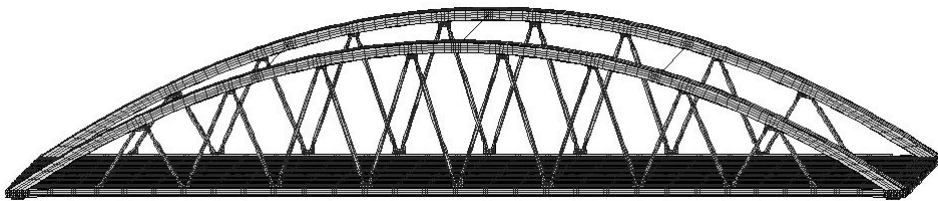

Figure 2: Finite element model of the Albert Canal Bridge.

2.1 The arches

Both of the arches of the bridge are stiffened using diaphragms and longitudinal stiffeners, at the connection of the arch with the hangers and at the connection of the arch with the tubular wind bracings.

The diaphragms at the connection with the hangers can be seen in Fig. 3 To allow for a better visibility of the diaphragms, one web plate has been removed from the model. In the lower flange plate of the arch, a longitudinal gap is designed, allowing the connection plate with the

hangers to enter the arch without connecting it to this flange of the arch, which would result in extreme local stresses. This connection plate also extends into the hangers, which have a rectangular shape. This plate introduces the hanger forces into the arch. The connection between the arch and the connection plate is made by two diaphragms, which are welded to both ends of the connection plate, which ensures that the hanger forces are transmitted to the arch cross-section as evenly as possible. These diaphragms also increase the resistance of the arch cross-section to distortion.

   Other stiffened sections are found at the connection with the tubular wind bracings. The wind bracing tubes are connected to the arch sections, and on both ends of these bracings, diaphragms are installed inside of the arch, as can be seen in Fig. 4. Again, I this figure one web plate of the arch section, as well as the wind bracing itself are removed to deliver a better view on the diaphragms. These two diaphragms are connected to each other by two additional longitudinal stiffeners.
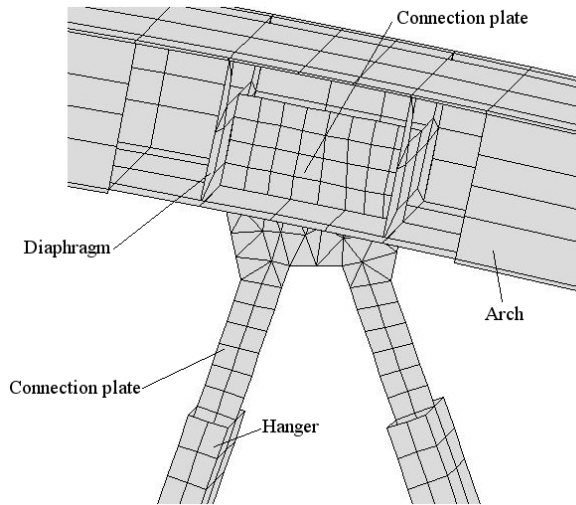

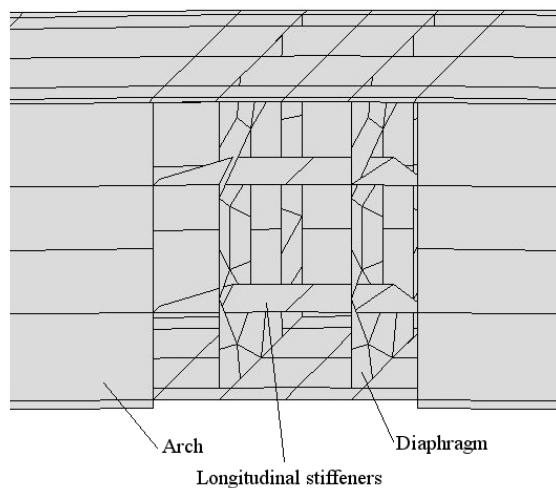Figure 3: Stiffening of the arch cross-section at the connection of the arch with the hangers.

Figure 4: Stiffening of the arch at the connection of the wind bracings.

2.2 Orthotropic plated bridge deck

Since the lower chord member of this steel tied-arch bridge consists of an orthotropic plated bridge deck, which has a very specific behaviour, the deck plate of the Albert Canal bridge is also modelled in detail, as can be seen in Fig 5. The longitudinal and transversal stiffness of the orthotropic plated deck are distribute the traffic loads forces to the arches by means of the hangers. For further clarification of the illustration of the bridge deck in Fig. 5, the deck plate has been removed, displaying the trapezoidal stiffeners and the crossbeams.

The lower chord of the arches consists of two longitudinal girders with an inverted T-cross section. These two girders are connected other by crossbeams. Furthermore, the deck plate is stiffened by 10 longitudinal closed section stiffeners. These stiffeners cross the crossbeams through special cut-outs in the webs, to avoid a very negative fatigue detail.

At the arch springs, the arch compression forces are introduced in the deck plate. The thickness of the bridge parts and especially the deck plate and crossbeam, is higher, the bridge deck being equipped with additional longitudinal and transversal stiffeners, as can be seen in Fig. 6.
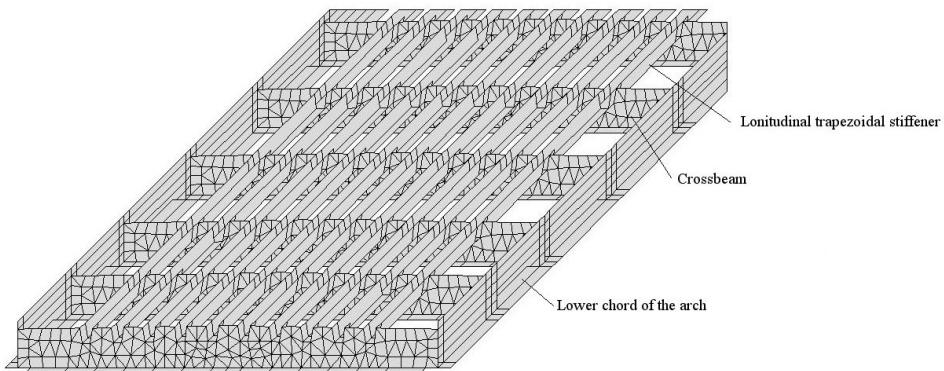

Figure 5: Cross section of the orthotropic plated bridge deck, showing the various stiffeners

2.3 The bearing systems and the arch springs

A first calculation run of the finite element model indicated that an important torsion effect exists near the arch springs, which fades out almost exponentially with increasing distance to the arch springs. This torsion effect is partly introduced by the neoprene bearings, which can be seen in Fig. 6. These bearings are not completely identical for the two arch springs, resulting in unsymmetrical end conditions. In addition, the neoprene bearing system, for which the movement is restrained in the transverse direction of the bridge, can still move a few millimetres in that direction. The same applies to the longitudinally and the fully restrained .This small freedom of movement allows the small deformations of the ends of the bridge deck to be transmitted to the arch springs, thus resulting in the torsion effect mentioned above. Obviously, a small portion of free displacements is indispensable to allow for the edge angular rotations, causing these small movements a various depth above the bearing centroid.

The modelling of these neoprene bearing systems necessitates the use of approximately 2000 volume elements of the Mindlin type. A series of specific flexible/flexible contact elements between the neoprene block with its steel interlayers and the fixing studs surrounding the neoprene block are used in the finite element model. For this application, a contact element has been created, which results in a kinematic constraint which is activated as soon as contact occurs between the surfaces of the relevant volume elements, but remains inactive when this contact condition does not appear.
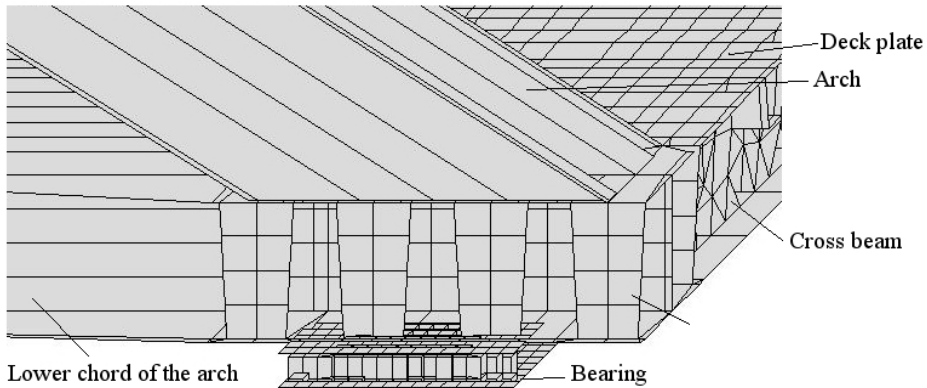
Figure 6: Detail of the arch spring and the supporting neoprene bearings.

Three types of calculations have been used for assessing the influence of restrained displacements by the bearings. At a first stage the boundary conditions of the bridge were forced to steel plates rigidly connected to the main beam lower flanges. The boundary conditions result from the displacements allowed by the bearings, loaded by the reactions from the bridge, being considered separately. During a second stage, the aforementioned steel plates are replaced by the elaborate numerical model of neoprene bearings using volume elements of the bearings

Finally a set of calculations assumes the neoprene bearings are being replaced by pot bearings. Each pot bearing is installed at the same location as its neoprene equivalent, the top plate having identical dimensions as the neoprene bearings.

2.4   Geometrical out-of-plane imperfections

As mentioned before, the possible out-of-plane imperfections are superposed on the actual arch geometry. All of the enforced imperfections show a single wave sinus curve, with maximum amplitude of 115 mm. This amplitude equals 1/1000 fraction of the total the arch span, which is the value recommended by the buckling curves from European Convention for Constructional Steelwork (1977).

The influence of the geometrical out-of-plane imperfections of both arches is also investigated. These calculations are performed, once for the case of both arches having identical imperfections in the same direction and once with both arches having imperfections with identical amplitudes, but in opposite directions.

2.5   Finite element model calculation strategy

The finite element model of the bridge is then used during two completely different types of calculations. Firstly, a linear elastic calculation is carried out, the load acting on the bridge being increased linearly and the calculation being stopped, if the displacements of the bridge become as large, any further increase would inevitably resulting in infinite increase of displacements. This situation corresponds to the elastic arch buckling. This calculation starts while having only the dead load of the structure. In the following time steps, the live load consisting of sixteen heavy lorries is placed on the bridge deck and is being increased stepwise. Starting from time step 2, the weight of these 16 lorries is increased linearly until the end of the calculation is reached by divergence of the finite element calculation criterion.

A subsequent calculation is of the elastic-plastic type. The calculation strategy is similar to the former one, using this time plastic material behaviour law for the steel parts of the structure. The definition of this material law complies to Eurocode guidelines for the finite element modelling of plastic materials.

These two types of calculations are then repeated for each type of bearing system and for all of the combinations of geometrical out-of-plane imperfections superposed on the arch geometry, according to the previous paragraph.

In order to calculate the buckling curves of the arches, supported by the three different types of bearing systems, as well as for all other calculations reported in this paper, this type of elastic-plastic analysis is preferred to more classical linear stability calculations for finite element software. The method allows for better distinguishing the increase of the lateral displacements with each increment of the vertical load on the bridge deck before reaching the bifurcation point. In contrast to linear stability analysis, material non linear analysis returns the exact value of the failure load of the construction. The difference in behaviour between an arch supported by neoprene bearings and by pot bearings thus becomes very clear. A second advantage of the procedure is that not all loads must be increased during the analysis, the dead load being held at constant value during the calculation process and the live load being stepwise increased. This incremental loading corresponds to actual buckling behaviour, rather than the application of increasing of the total load.

3 USE OF BUCKLING CURVES FOR ELASTIC-PLASTIC CONDITION

Eurocode, EN 1993-1-1(2005) or the ECCS-curves do not give a specific buckling curve for arches. Since the arch section of the Albert Canal Bridge is a rectangular welded box, buckling curve b should be used for the design of this arch bridge, although this buckling curve was developed for the design of straight beams and columns.

For each type of bearing system, as well as for each type of enforced imperfection, the critical elastic normal force and the critical plastic normal force in the arch cross-section were determined using the finite element model described above. The appropriate dimensionless slenderness was calculated using the critical elastic normal force, N_{cr}, as can be seen in Eq. (1). Herein A is the area of the cross-section of the arch and f_y the yield strength.

$$\overline{\lambda} = \sqrt{\frac{A \cdot f_y}{N_{cr}}} \tag{1}$$

The critical plastic normal force, N_u, could then be used to calculate the buckling factor:

$$v_u = \frac{N_u}{A \cdot f_y} \tag{2}$$

4 CALCULATION RESULTS, RELATIVE TO THE BUCKLING CURVES

4.1 Geometrical imperfections

The results of the finite element calculations, for the model with several types of imperfections are shown in Fig. 7. For each calculation, the post processing and subsequent calculation of the normal forces is always performed for the same arch, called "Arch I", the opposite arch logically being called "Arch II".

All of the calculation results are located well above buckling curve b, which according to EN 1993-1-1 has to be used for the design of this arch bridge. It can thus be stated, that calculation of arch stability based on the assumption that buckling curve b for linear elements is valid for arched elements, is conservative. In fact the buckling load will be much higher, closer to the value obtained from buckling curve a_0. Since no specific buckling curves for arches exist at this present, this situation cannot be avoided.

Both of the following figures also plot the limit value, as well as the most relevant buckling curves of the Eurocode, EN 1993-1-1 (2005) , to allow for comparison.
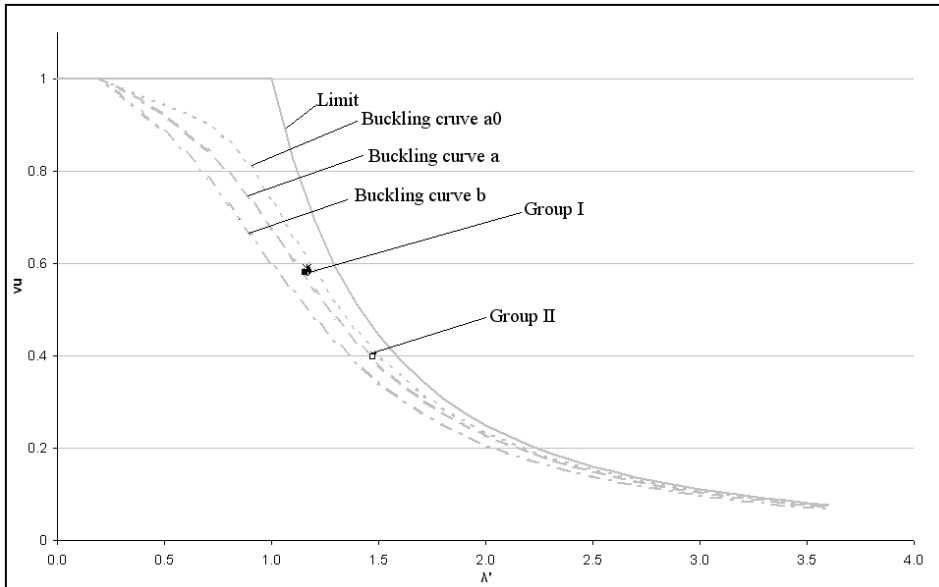
Figure 7: Influence of the geometrical out-of-plane imperfections on the buckling behaviour, relative to the buckling curves.

All of the calculation results are divided into two groups of points in Fig. 7. Group I corresponds to perfect arch behaviour of "Arch I", or to the "Arch I" condition with half sine wave imperfections having 115 mm amplitude. This amplitude is directed towards the second arch of the bridge. Group II, in Fig 7 displays all calculation results for "Arch I" having half sine wave imperfections of -115 m amplitude, which is directed away form the opposite arch. The exception to this rule are the data points, for which both of the arches have imperfections in opposite directions, or in other words, when both arches bend towards each other or away from each other. In the condition of "Arch I" showing a negative imperfection, e.g. directed away form "Arch II" and at the same time "Arch II" showing an imperfection directed towards "Arch I", the calculation result is located in group I, and not in group II. In general, it can be concluded that the imperfections of the arch, the buckling behaviour of which is being studied, are determining the buckling load.

4.2 Influence of the bearing systems

For each type of bridge bearing system discussed above, the values of the buckling factor and of the slenderness are plotted in the diagram of the buckling curves, as defined in the Eurocode, as displayed in Fig. 8.

The results for each type of bridge bearing are all located well above buckling curve b. This abundantly demonstrates that should arch bridges be designed by using buckling curve b for linear elements the result will be too conservative, the real condition being closer to the result from buckling curve a_0.

This calculation draws attention to the importance of the type of bearings supporting steel tied-arch bridges. Pot bearings render improved buckling loads and stability behaviour compared to neoprene bearings, as can be clearly seen on Fig. 8.
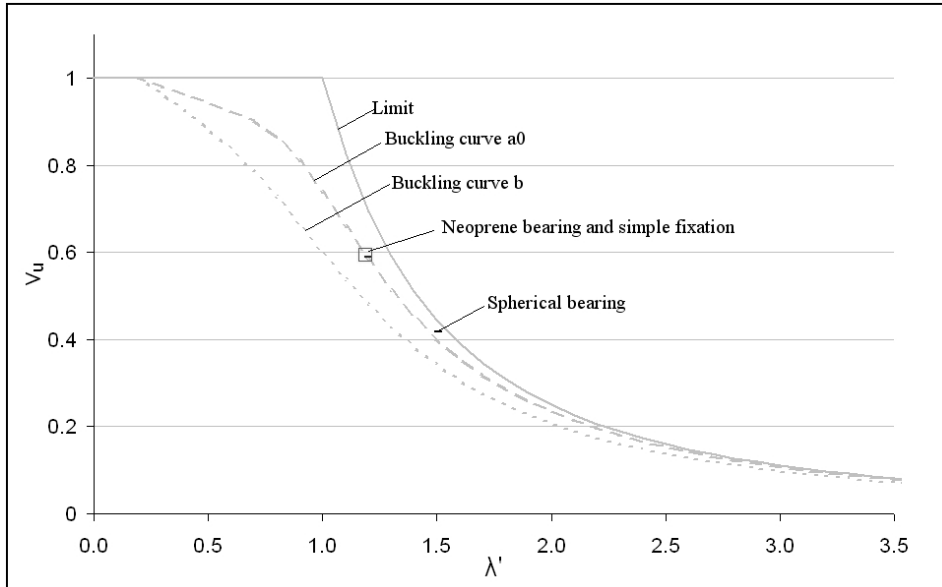
Figure 8: Influence of the type of bearing on the buckling behaviour of an arch.

5   CONCLUSION

An elaborately detailed finite element model of a steel tied-arch bridge is used to assess the influence of bearing systems on the buckling behaviour of the arch, including out-of-plane geometrical imperfections.

A perfect steel tied-arch bridge, supported by pot or neoprene bearings has higher buckling resistance than a straight beam, having identical cross-section characteristics.

Regardless of the influence of the bearing systems, it has been implied that the shape and the direction of the geometrical out-of-plane imperfections are determining the buckling behaviour of the arch.

Finally, apart from geometrical imperfections, the bearing systems have an important part in the buckling behaviour of arches. A steel tied-arch bridge supported by pot bearings shows higher buckling resistance than in case of having a neoprene bearing system.

REFERENCES

ECCS-EG77-2E, 1978, *European Recommendations for Steel Construction* European Convention for Constructional Steelwork.

European convention for Constructional Steelwork, Tokyo 1976, Liege 1977, Washington 1977, *Manual on the stability of steel structures*, Puteaux (Paris)

Outtier, A., De Backer, H. and Van Bogaert, Ph. 2006 *Lateral buckling of a steel tied-arch*. In 10th East Asia Pacific conference on Structural Engineering & Construction, 3-5 Augustus 2006, Bangkok, Vol. 4: Real Structures and Tall Buildings, pp 275-280 (CD-ROM).

EN 1993-1-1, 2005, *Eurocode 3: Design of steel structures*, CEN, Brussels, pp. 344.

Van Bogaert Ph. and Outtier A.,2006, *Strain Measurements as a Tool for Stability Verification of Steel Tied-arches*, Proc. Int. Conference on Bridges SECON, Ed Radic, J. Secon HDGK, Dubrovnik, pp. 1043-1050